

Rigorous Strip Adjustment of UAV-based Laserscanning Data Including Time-Dependent Correction of Trajectory Errors

Philipp Glira, Norbert Pfeifer, and Gottfried Mandlburger

Abstract

A new generation of laser scanners mounted on Unmanned Aerial Vehicles (UAVs) have the potential to provide high-quality point clouds of comparatively small areas (a few hectares). The high maneuverability of the UAVs, a typically large field of view of the laser scanners, and a comparatively small measurement range lead to point clouds with very high point density, less occlusions, and low measurement noise. However, due to the limited payload of UAVs, lightweight navigation sensors with a moderate level of accuracy are used to estimate the platform's trajectory. As a consequence, the georeferencing quality of the point clouds is usually sub-optimal; for this, strip adjustment can be performed. The main goal of strip adjustment is to simultaneously optimize the relative and absolute orientation of the strip-wise collected point clouds. This is done by fully re-calibrating the laser scanning system and by correcting systematic measurement errors of the trajectory. In this paper, we extend our previous work on the topic of strip adjustment by the estimation of time-dependent trajectory errors. The errors are thereby modelled by natural cubic splines with constant segment length in time domain. First results confirm the suitability of this flexible correction model by reducing the relative and absolute strip discrepancies to 1.38 cm and 1.65 cm, respectively.

Introduction

Airborne Laser Scanning (ALS) from *manned* platforms is a widely used and proven technology for the acquisition of point clouds over extended areas. Recent developments created the possibility to mount lightweight laser scanners, together with the required navigation sensors, on Unmanned Aerial Vehicles (UAVs), whereby small multicopter systems are typically used. Though such systems are restricted to the mapping of smaller areas, they have the potential to deliver high-quality point clouds, i.e., point clouds with very high and homogeneous point density, footprint diameters of just a few centimeters, minimal occlusions, and low measurement noise (Mandlburger *et al.*, 2015a).

While the usage of imaging sensors on UAVs is already widespread in many research fields, the application of laser scanners on UAVs is still less common and remains challenging (Colomina, 2015). One of the main reasons is that, in contrast to frame based imaging systems, such dynamic laser scanning systems require a continuous and accurate estimate of the flight trajectory. This is particularly challenging for UAVs, as they typically have highly variable flight dynamics, can be subject to strong vibrations, and satellite visibility may be restricted at very low flying altitudes or when flying between tall buildings or vegetation. Due to the limited payload

of UAVs, lightweight navigation sensors with a moderate level of accuracy have to be used, resulting in a comparatively weak estimation of the trajectory. Despite the low flying altitude of UAVs, which is advantageous for the propagation of angular errors on the point clouds' georeference, the estimated trajectory usually cause time-dependent, non-linear deformations of the strip-wise collected point clouds. To correct these deformations and thereby optimize the georeferencing of the point clouds, *strip adjustment* can be performed. In Figure 1 the point clouds captured from different flight strips are shown for a small wooded area. A horizontal profile through the stems of a tree clearly demonstrate the improved alignment of the point clouds after strip adjustment.

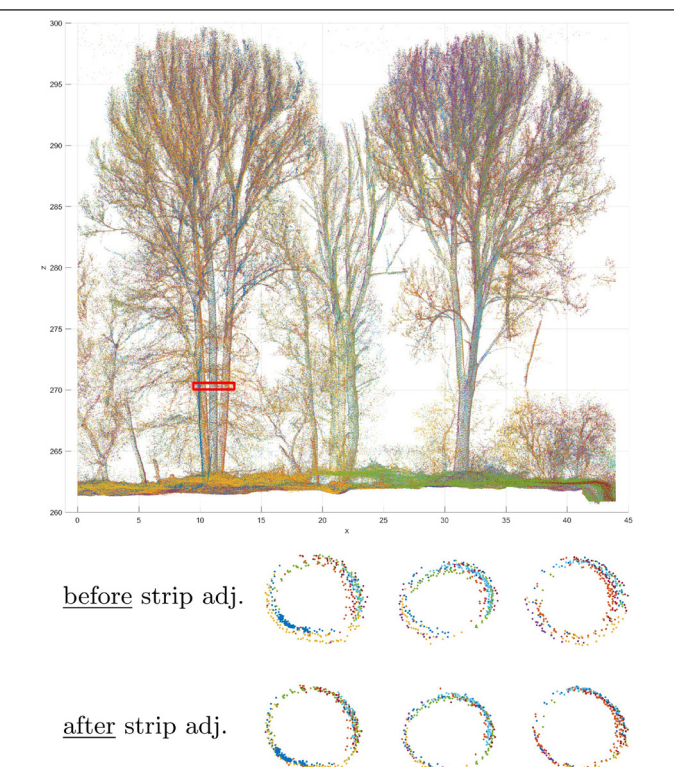


Figure 1. Top: Point cloud captured during an ALS campaign after strip adjustment (different colors correspond to different flight strips). Below: horizontal section through the stems of a tree (height = 0.5 m) before and after strip adjustment.

Photogrammetric Engineering & Remote Sensing
Vol. 82, No. 12, December 2016, pp. 945–954.
0099-1112/16/945-954

© 2016 American Society for Photogrammetry
and Remote Sensing
doi: 10.14358/PERS.82.12.945

The typical point cloud generation process for *dynamic* laser scanning systems is depicted in Figure 2. It starts from the key components of the navigation system, a Global Navigation Satellite System (GNSS) and an Inertial Navigation System (INS). The measurements of these systems are integrated in some sort of Kalman filter (Kalman, 1960) to produce an accurate estimate of the platforms' trajectory, i.e., its position (three coordinates: x, y, z) and orientation (three angles: roll, pitch, yaw) as a function of time. The so-obtained trajectory is combined with the mounting calibration parameters (which describe the positional and rotational offsets between the scanner and the GNSS/INS system) to determine the orientation of the laser scanner (*direct sensor orientation*). Finally, the measurements of the laser scanner can be directly georeferenced to obtain the final product, the georeferenced point clouds.

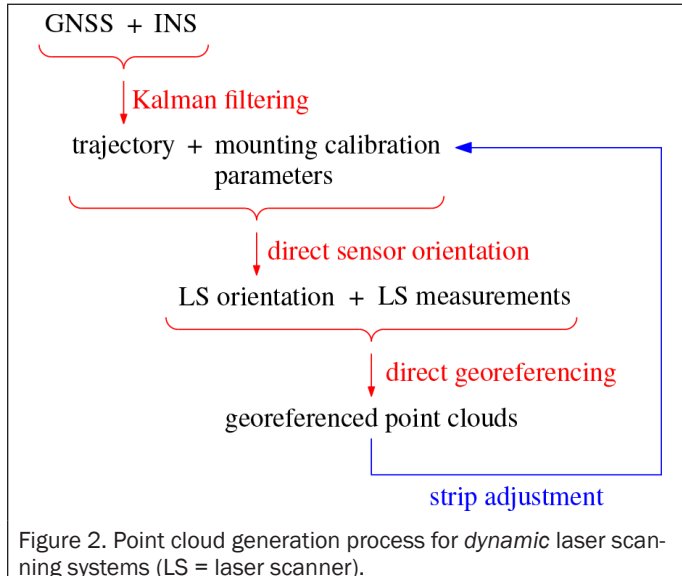


Figure 2. Point cloud generation process for *dynamic* laser scanning systems (LS = laser scanner).

In many cases, the so-generated point clouds contain systematic georeferencing errors. These errors can be recognized in two forms: (a) as discrepancies between overlapping strips, and (b) as discrepancies between strips and ground-truth data, e.g., ground control points or reference planes. Experience shows, that the major parts of these discrepancies stem from the GNSS/INS navigation system and from the rotational part of the mounting calibration (*boresight misalignment*). To re-calibrate the entire ALS multisensor system and correct the trajectory errors, strip adjustment (also known as *integrated sensor orientation*) can be performed. This is done by refining the point cloud generation process *after* the trajectory estimation by additional (calibration and correction) parameters. These parameters are estimated by exploiting the redundancy contained in the overlapping areas of the strips and by considering ground-truth data (if available). The estimated parameters can be divided into three categories: (a) the scanner calibration parameters (e.g., range finder offset), (b) the mounting calibration parameters (lever-arm and misalignment), and (c) the trajectory correction parameters. In this article, we focus on the latter.

To our best knowledge, trajectory estimation and laser scanning strip adjustment are always treated as two independent problems: the Kalman filter does not consider any laser scanner observations and strip adjustment in turn does not consider any raw observations of the GNSS/INS navigation system (e.g., pseudorange and carrier phase observables). In other words, sensor calibration and error modeling are not integrated on the highest possible level. Such a solution is

undoubtedly suboptimal, but it splits a complex problem into two smaller, easier manageable problems. As a consequence of this separation, the errors of the raw GNSS/INS observations cannot be corrected directly by strip adjustment. Instead, the effect of these errors on the trajectory estimation must be modeled. As the GNSS and INS measurements are strongly affected by external influences (e.g., satellite constellation, flight maneuvers), these errors cannot be assumed to be constant in time, but strongly time-dependent (Skaloud, *et al.*, 2010).

The simplest trajectory error model is a bias correction (by 0-degree polynomials) for each of the six trajectory elements, individually for each strip (Glira *et al.*, 2015b); we call this the *bias trajectory correction model* throughout this paper. Other models additionally can mitigate the effect of linear and quadratic INS drifts (by 1- or 2-degree polynomials), although such drifts should already be corrected to a large extent in the Kalman filter by other measurements, especially GNSS measurements (Colomina, 2015). Due to its simplicity, these correction models are often insufficient. This is particularly the case when:

- A very high georeferencing accuracy is demanded, e.g., for deformation monitoring or modeling of complex objects like buildings or trees (Figure 1).
- The accuracy of the navigation sensors exceed the laser scanner's accuracy, i.e., the trajectory is the dominant error source for the final georeferencing accuracy of the point clouds.
- The trajectory estimation was not performed in a proper way, and therefore contains large errors.

This paper presents a new and flexible correction model, which can be used to estimate time-dependent trajectory errors and can be incorporated easily into the functional model of a rigorous strip adjustment method. Thereby, errors are modeled individually for each of the six trajectory elements by smoothed, piecewise-defined cubic polynomials, commonly known as cubic splines; this model is hereinafter referred to as *spline trajectory correction model*.

The remainder of the paper is structured as follows. After a review of literature in the next section, the fundamentals of our strip adjustment method are briefly summarized. On this basis, a detailed description of the *spline trajectory correction model* is provided and the first results are presented. A critical review of the method is presented in the last section.

Related Work

Trajectory correction (or estimation) is a research topic not only in the domain of laser scanning, but also in many other research areas where *dynamic* measurement systems (a.k.a., mobile mapping systems) are used. A state-of-the-art overview about trajectory estimation for photogrammetry and remote sensing applications has been recently published by Colomina (2015). In the following, some works particularly related to the estimation of trajectory errors, are presented.

Airborne Laser Scanning

Most strip adjustment methods presented in the past concentrate on the estimation of the three boresight misalignment angles, e.g., Hebel and Stilla (2012). The reasons for this are that (a) these angles are difficult to observe by conventional surveying methods, and (b) angular errors can cause very large point displacements, as their effect is directly proportional to the measurement range. Obviously, the latter applies also to the orientation angles roll, pitch, and yaw. In Kager (2004) each trajectory element can be corrected strip-wise by a single polynomial of arbitrary degree. Friess (2006) presents an extensive framework for strip adjustments which includes the correction of trajectory errors, without however, providing

further details about the utilized error model. An overview of UAV-suitable laser scanners and navigation sensors can be found in Colomina and Molina (2014). A general overview about strip adjustment methods, including a discussion of potential random and systematic error sources and their effect on the ground points, can be found in Habib *et al.*, (2009).

Mobile Laser Scanning

Colomina (2015) emphasizes that in contrast to ALS, MLS is usually performed in less responsive GNSS environments, where, due to obstructions, signal attenuation, and multipath, systematic errors of 0.5 m and larger are common. However, only few studies have been conducted on the correction of these errors in the past. Nolan *et al.* (2015) recently presented a trajectory correction method, which can be applied to point clouds acquired in multiple passes (loops). Within the overlap area of these point clouds, a so-called “control polyline” is extracted along the trajectory (e.g., a curb). This 3D polyline is incorporated into a least squares adjustment to improve the given trajectory. Nuechter *et al.* (2015) use a 2D and a 3D scanner, mounted together on a backpack, to map indoor environments without any navigation sensors, i.e., without GNSS and INS. It is demonstrated that using Simultaneous Localization and Mapping (SLAM), the acquired point clouds can be referenced in a common coordinate system, although the reported accuracy of the point clouds lies in the “centi/decimeter range” only.

Three-Line Cameras

Due to their high image acquisition frequency, three-line cameras (Hofmann *et al.*, 1984) need a continuous trajectory estimate. In contrast to our work, Ebner *et al.* (1992) do not estimate the *errors* of a given trajectory, but the trajectory itself. For this reason, the exterior orientation for some image lines at certain time intervals is estimated. Between these images, the trajectory is interpolated by Lagrange polynomials of third degree. In Gruen and Zhang (2002) the orientation angles are corrected by bias and drift parameters. A more flexible model is presented for the position coordinates, which are corrected by piecewise second-degree polynomials with continuity constraints.

Strip Adjustment Method

The basics of the strip adjustment method applied in this study were previously published in two articles: Glira *et al.* (2015a) concentrates on the definition and selection of correspondences, whereas Glira *et al.* (2015b) provides a framework for the entire strip adjustment method. As a basis for the remainder of this article, the fundamentals of these two articles are summarized in the following.

Rigorous Modeling of the Measurement Process

Some strip adjustment methods use the 3D coordinates of the point clouds only as data input (e.g., the provided .las files) (e.g., Ressl *et al.* (2011); Vosselman and Maas (2001)). In our method, however, the generation of the point clouds is rigorously modeled by considering (a) the original scanner measurements, (b) the mounting calibration, and (c) the trajectory measurements. For the generation of the point clouds, these inputs are combined in the direct georeferencing equation (Glira *et al.*, 2015b):

$$\mathbf{x}^e(t) = \mathbf{g}^e(t) + R_n^e(t)R_i^n(t)(\mathbf{a}^i + R_s^i \mathbf{x}^s(t)) \quad (1)$$

where $\mathbf{x}^e(t)$ is a 3-by-1 vector with the coordinates of the laser point measured at time t . The indices in Equation 1 denote the following coordinate systems (Bäumker and Heimes, 2001):

- s -system scanner coordinate system
- i -system INS coordinate system (often also denoted as body coordinate system)
- n -system navigation coordinate system, equal to a local-level coordinate system ($x = \text{north}$, $y = \text{east}$, $z = \text{nadir}$)
- e -system Earth-Centered, Earth-Fixed (ECEF) coordinate system.

Furthermore Equation 1 includes:

- $\mathbf{x}^s(t)$ 3-by-1 vector with the coordinates of the laser point in the s -system.
- R_s^i 3-by-3 rotation matrix describing the rotation from the s -system to the i -system. This rotation is usually denoted as (boresight) misalignment and is parametrized through three Euler angles:

$$R_s^i = R_s^i(\omega, \phi, \kappa) \quad (2)$$

- \mathbf{a}^i 3-by-1 vector describing the positional offset between the GNSS antenna and the origin of the s -system. This vector is usually denoted as lever arm.
- $R_i^n(t)$ 3-by-3 rotation matrix describing the rotation from the i -system to the n -system. This rotation is parameterized through three Euler angles roll ϕ , pitch θ , and yaw ψ :

$$R_i^n(t) = R_i^n(\phi(t), \theta(t), \psi(t)) \quad (3)$$

- $R_n^e(t)$ 3-by-3 rotation matrix describing the rotation from the n -system to the e -system. This rotation is not observed, but is a function of the longitude λ and latitude φ corresponding to the actual value of $\mathbf{g}^e(t)$:

$$R_n^e(t) = R_n^e(\lambda(t), \varphi(t)) \quad (4)$$

- $\mathbf{g}^e(t)$ 3-by-1 vector describing the position of the GNSS antenna in the e -system.

Calibration of the ALS Multisensor System

For an on-the-job calibration of the entire ALS system, the direct georeferencing equation is extended by additional calibration parameters. These parameters are estimated by strip adjustment and include calibration parameters for the scanner and the mounting calibration parameters (*misalignment* and *lever-arm*).

Correction of Aircraft's Trajectory

Up to now, we used a rather simple correction model for the aircraft's trajectory: only the biases of each trajectory element (three coordinates, three angles) were estimated individually for each strip¹ (*bias trajectory correction model*). However, these six parameters per strip are insufficient if the input trajectory is of poor quality or if a very high georeferencing quality is required. In such cases, a more flexible trajectory correction model is required, which is the focus of this study and will be presented in the next section.

Point Based Correspondences

In order to exploit the full resolution of the data, correspondences are established on the basis of the original ALS points. For the spatial selection of correspondences within the overlap area of the strips, four different selection strategies were presented in Glira *et al.* (2015): (a) Random Sampling,

1. If a very accurate trajectory is provided, it might be sufficient to estimate the biases block-wise only (instead of strip-wise). However, in our experience this is very rarely the case.

(b) Uniform Sampling, (c) Normal Space Sampling, and (d) Maximum Leverage Sampling. A single correspondence is defined by two closest points and their normal vectors. Between these two points, the signed point-to-plane distance (Figure 3) is minimized. It is conveniently expressed by

$$d_i = (\mathbf{p}_i - \mathbf{q}_i)^T \mathbf{n}_i \quad (5)$$

where \mathbf{p}_i and \mathbf{q}_i are the corresponding points of the i^{th} correspondence, and \mathbf{n}_i is the normal vector associated to the point \mathbf{p}_i (with $\|\mathbf{n}_i\| = 1$).

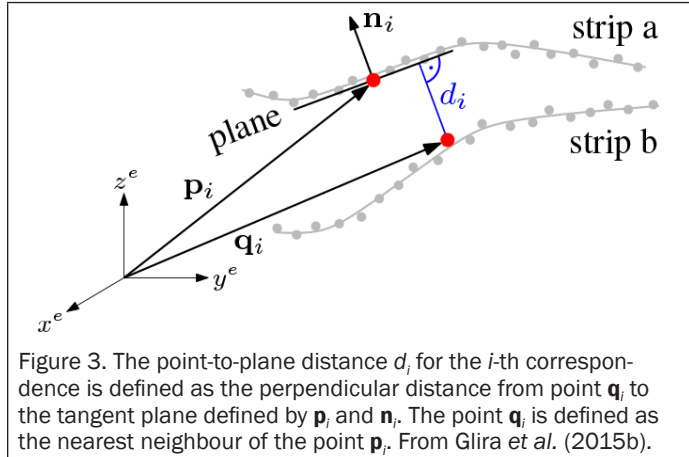


Figure 3. The point-to-plane distance d_i for the i^{th} correspondence is defined as the perpendicular distance from point \mathbf{q}_i to the tangent plane defined by \mathbf{p}_i and \mathbf{n}_i . The point \mathbf{q}_i is defined as the nearest neighbour of the point \mathbf{p}_i . From Glira et al. (2015b).

Objective of the Adjustment

A robust least squares adjustment (*Gauß-Markov adjustment model*) is performed to estimate the unknown calibration and trajectory correction parameters. The objective of the adjustment is to simultaneously minimize the weighted sum of all squared point-to-plane distances

$$\Omega = \sum_{i=1}^n (w_i d_i^2) \rightarrow \text{minimum} \quad (6)$$

where d_i is the point-to-plane distance of the i^{th} correspondence, w_i its weight, and n the total number of correspondences. The definition of the weights is given in Glira et al., (2015b).

Iterative Estimation

Correspondences are not established only once, but iteratively. For each new set of correspondences, the parameters are re-estimated through adjustment. This iterative procedure is repeated until convergence is reached, i.e., until there are no significant changes in the estimated parameters. Hence, the strip adjustment method is partly based on the well-known Iterative Closest Point (ICP) algorithm (Besl and McKay (1992), Chen and Medioni (1992)).

Spline Trajectory Correction Model

The trajectory of the platform is estimated in advance by the integration of GNSS and INS measurements in a Kalman filter. As a result, the position and the orientation estimates are given, together with their precisions, as a function of the flight time t :

Original position	Original orientation
$g_{x0}^e(t)$...x-coordinate	$\phi_0(t)$...roll angle
$g_{y0}^e(t)$...y-coordinate	$\theta_0(t)$...pitch angle
$g_{z0}^e(t)$...z-coordinate	$\psi_0(t)$...yaw angle

We use here the same notation as in Glira et al. (2015b). The superscript e indicates that the position is expressed in an Earth-Centered, Earth-Fixed (ECEF) coordinate system (previous section). Each of these six trajectory elements is corrected, individually for each strip j , by a correction function $\Delta(t)$:

Corrected position	Corrected orientation
$g_x^e(t) = g_{x0}^e(t) + \Delta g_{x[j]}^e(t)$	$\phi(t) = \phi_0(t) + \Delta\phi_{[j]}(t)$
$g_y^e(t) = g_{y0}^e(t) + \Delta g_{y[j]}^e(t)$	$\theta(t) = \theta_0(t) + \Delta\theta_{[j]}(t)$
$g_z^e(t) = g_{z0}^e(t) + \Delta g_{z[j]}^e(t)$	$\psi(t) = \psi_0(t) + \Delta\psi_{[j]}(t)$

In this paper, we investigate the usage of **natural cubic splines with constant segment length Δt in time domain** for modeling these correction functions (Figure 4). This model choice is inevitably somewhat arbitrary, as the true pattern of the residual trajectory errors is unknown. However, using cubic splines has some justifiable grounds:

- The residual trajectory errors are expected to be smoothed in forward and backward direction after Kalman filtering. Due to their smoothness and high flexibility, cubic splines are an appropriate counterpart to the long-term components of these residual errors.
- In comparison with higher-degree polynomials, the risk of overfitting is relatively small for cubic splines. However, if a too small segment length Δt (e.g., 0.5 s) is chosen, overfitting may still occur.
- Due to their straightforward mathematical formulation, cubic splines can be easily incorporated (together with the appropriate constraints) into the functional model of an adjustment.

Correction Model

This section contains the equations required for the incorporation of the proposed correction model into the adjustment. It is emphasized that an individual correction function is estimated for each trajectory element and for each flight strip j ($j = 1, \dots, s$). If we denote the start and end time of the j^{th} strip with $t_{s[j]}$ and $t_{e[j]}$ respectively, the total number of polynomial segments for each trajectory element of this strip is defined by

$$n_{[j]} = \left\lceil \frac{t_{e[j]} - t_{s[j]}}{\Delta t} \right\rceil \quad (7)$$

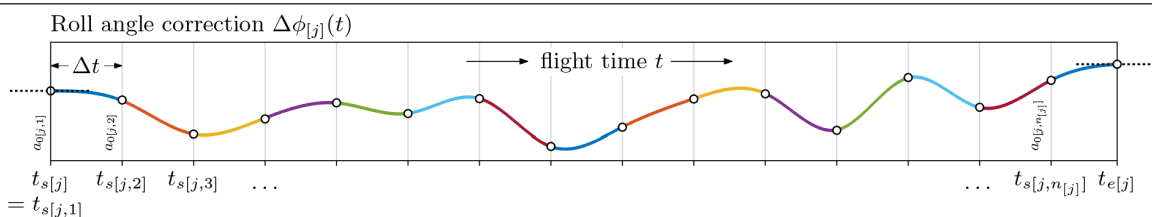


Figure 4. Example of roll angle correction for a single flight strip j . The correction is modeled as natural cubic spline with constant segment length Δt . At the beginning and the end of a strip, the first and second derivatives are constrained to zero. The continuity and smoothness of the spline function are ensured by the C^0 , C^1 , and C^2 continuity constraints.

where Δt is the segment length of a single polynomial in time domain. The k^{th} cubic polynomial ($k = 1, \dots, n_{[j]}$) of the j^{th} strip is represented, e.g., for the roll angle correction, by:

$$\begin{aligned}\Delta\phi_{[j,k]}(t) = & a_{0[j,k]} \\ & + a_{1[j,k]}(t - t_{s[j,k]}) \\ & + a_{2[j,k]}(t - t_{s[j,k]})^2 \\ & + a_{3[j,k]}(t - t_{s[j,k]})^3\end{aligned}\quad (8)$$

whereby the start time of the polynomial is:

$$t_{s[j,k]} = t_{s[j]} + (k - 1) \cdot \Delta t \quad (9)$$

and the polynomial is defined for the time interval:

$$\begin{aligned}\text{for } k = 1, \dots, n_{[j]} - 1 & \rightarrow t \in [t_{s[j,k]}, t_{s[j,k+1]}] \\ \text{for } k = n_{[j]} & \rightarrow t \in [t_{s[j,k]}, t_{e[j]}]\end{aligned}$$

However, if the last polynomial is very short, e.g., smaller than $\Delta t/2$, it should be merged with the previous one.

The coefficients $a_{0[j,k]}$, $a_{1[j,k]}$, $a_{2[j,k]}$, and $a_{3[j,k]}$ of each polynomial (Equation 8) are estimated by adjustment. A summary of all unknown parameters, including those previously described in Glira *et al.* (2015b), can be found in Table 1.

Table 1. Overview of the parameters estimated by strip adjustment. The estimation of the scanner and mounting calibration parameters has been previously described in Glira *et al.* (2015b)

Parameters		
category	name	#
scanner	range offset (bias)	1
	range scale	1
calibration	angle offsets (biases)	2
	angle scales	2
mounting calibration	misalignment angles	3
	lever-arm components	3
trajectory correction	x correction coefficients	$4\sum_{j=1}^s n_{[j]}$
	y correction coefficients	$4\sum_{j=1}^s n_{[j]}$
	z correction coefficients	$4\sum_{j=1}^s n_{[j]}$
	roll correction coefficients	$4\sum_{j=1}^s n_{[j]}$
	pitch correction coefficients	$4\sum_{j=1}^s n_{[j]}$
	yaw correction coefficients	$4\sum_{j=1}^s n_{[j]}$

Constraints

To ensure that the splines are continuous and smooth at the junctions of the polynomials, the following constraints have to be incorporated for the inner knots ($k = 1, \dots, n_{[j]} - 1$) into the adjustment:

- the **C⁰ continuity** expresses that the polynomials are continuous at the internal knots:

$$\Delta\phi_{[j,k]}(t_{s[j,k+1]}) = \Delta\phi_{[j,k+1]}(t_{s[j,k+1]}) \quad (10)$$

- the **C¹ continuity** expresses that the first derivative of the polynomials is continuous at the internal knots:

$$\Delta\phi'_{[j,k]}(t_{s[j,k+1]}) = \Delta\phi'_{[j,k+1]}(t_{s[j,k+1]}) \quad (11)$$

- The **C² continuity** expresses that the second derivative of the polynomials is continuous at the internal knots:

$$\Delta\phi''_{[j,k]}(t_{s[j,k+1]}) = \Delta\phi''_{[j,k+1]}(t_{s[j,k+1]}) \quad (12)$$

The required first and second derivatives of Equation 8 are:

$$\begin{aligned}\Delta\phi'_{[j,k]}(t) = & a_{1[j,k]} \\ & + 2a_{2[j,k]}(t - t_{s[j,k]}) \\ & + 3a_{3[j,k]}(t - t_{s[j,k]})^2\end{aligned}\quad (13)$$

$$\begin{aligned}\Delta\phi''_{[j,k]}(t) = & 2a_{2[j,k]} \\ & + 6a_{3[j,k]}(t - t_{s[j,k]})\end{aligned}\quad (14)$$

Additionally, boundary conditions are introduced to avoid steep slopes of the correction function at the beginning and at the end of each flight strip (Figure 4). This is accomplished by setting the first and second derivatives to zero at the beginning ($t = t_{s[j]} = t_{s[j,1]}$) of each strip

$$\Delta\phi'_{[j,1]}(t_{s[j]}) = 0 \Rightarrow a_{1[j,1]} = 0 \quad (15)$$

$$\Delta\phi''_{[j,1]}(t_{s[j]}) = 0 \Rightarrow a_{2[j,1]} = 0 \quad (16)$$

and at the end ($t = t_{e[j]}$) of each strip

$$\Delta\phi'_{[j,n_{[j]}]}(t_{e[j]}) = 0 \quad (17)$$

$$\Delta\phi''_{[j,n_{[j]}]}(t_{e[j]}) = 0 \quad (18)$$

Equations 10, 12, 15, 16, 17, and 18 are incorporated as constraints into the adjustment; a summary is given in Table 2. The solution formulas for the applied *Gauß-Markov adjustment model with functionally dependent parameters* can be found in Mikhail and Ackermann (1976, p. 213).

Table 2. Overview for the constraints used in the adjustment

Constraints		
category	name	#
trajectory correction	C ⁰ , C ¹ , C ² continuity	$3 \cdot 6 \sum_{j=1}^s (n_{[j]} - 1)$
	boundary conditions	4·6s

Additional Observations

If a single strip is not fully overlapping with other strips, some polynomials cannot be estimated due to lack of correspondences. As a consequence the equation system becomes singular. To overcome this problem, fictional observations (sometimes also denoted as zero-observations) are added for the 0-degree polynomial coefficients $a_{0[j,k]}$ to the equation system. They have the form:

$$a_{0[j,k]} = 0 + v_{[j,k]} \quad (19)$$

where $v_{[j,k]}$ denotes the residual of the observation. As *a priori* precision of these observations $\sigma_{a_{0[j,k]}}$ the trajectory precision estimates from the Kalman filter should be used. If this information is not available, the measurement precisions, as declared by the manufacturers, can be used alternatively (Table 3). Besides removing the rank deficiency, these observations have also another important effect: they ensure that the trajectory correction functions converge steadily to zero in areas without redundancy, i.e., in areas without overlap. The original objective function (Equation 6) of the strip adjustment changes due to the additional observations to:

$$\Omega = \sum_{i=1}^n (w_i d_i^2) + \sum_{j=1}^s \sum_{k=1}^{n_{[j]}} (w_{[j,k]} a_{0[j,k]}^2) \rightarrow \text{minimum} \quad (20)$$

Table 3. Key features of the deployed measurement system as declared by the manufacturers

Measurement system	
laser scanner	model Riegl VUX-1UAV
	pulse repetition rate 350 kHz
	range accuracy 10 mm
	range precision 5 mm
	scan angle resolution 0.001°
	field of view 230°
	beam divergence 0.5 mrad
GNSS/INS	wavelength 1550 nm
	model Trimble Applanix AP20
	roll accuracy 0.015°
	pitch accuracy 0.015°
	yaw accuracy 0.035°
UAV	position accuracy 5-30 cm
	INS sampling rate 200 Hz
UAV	model Riegl RiCopter
	max. payload 16 kg
	max. flight time 30 min
	size 192 × 182 × 47 cm

where s denotes the total number of strips, and the weight $w_{[j,k]}$ is defined by

$$w_{[j,k]} = \frac{1}{\sigma^2_{a_{0[j,k]}}} \quad (21)$$

It should be noted that no additional observations are needed for the remaining coefficients $a_{1[j,k]}$, $a_{2[j,k]}$, and $a_{3[j,k]}$, as their determination is ensured by the constraints described in the previous section.

Possible Problems

Some problems may arise by using the *spline trajectory correction model*:

Absolute Deformation of the ALS Block

Due to the high flexibility of the trajectory correction model, systematic discrepancies between overlapping strips can

almost completely be eliminated, especially if a small segment length Δt is used. However, an absolute deformation of the whole ALS block might occur if Δt is too small (model overfitting), as in such cases the estimated trajectory correction parameters compensate not only trajectory errors, but also the effect of other error sources (e.g., a erroneous calibrated laser scanner). Thus, an appropriate choice of Δt is very important and will be discussed on the basis of real data in the next section. Alternatively, block deformations can also be avoided – almost independent from the actual choice of Δt – by using a large number of ground control points that are homogeneously distributed over the whole block.

Local Effect of Ground Control Points

Usually, single ground control points can be used to correct the datum of the whole ALS block. However, by using a time-dependent trajectory correction model, such widely isolated points have a local effect only, i.e. the datum is corrected in the vicinity of these points only. Since this problem is closely related to the previous one, it can also be avoided by using a dense network of ground control points.

Determinability of Trajectory Correction Functions

For a reliable estimation of the time-dependent trajectory correction functions, a dense and homogeneous distribution of the correspondences is needed. Furthermore, the determinability of the correction functions depends on the terrain geometry, and can therefore not be guaranteed in any case, e.g., over completely featureless, flat terrain; however, practical experience has shown that this is a rather theoretical problem.

Experimental Results

The study site Neubacher Au is a Natura2000 protection area located at the lower course of the Pielach River (Lower Austria) near the confluence with the Danube River (48°12'50" N, 15°22'30" E; WGS 84). Due to the complex topography and vegetation structure, the alluvial area was captured under leaf-off conditions by a Unmanned Aerial Vehicle (UAV)- mounted laser scanner (Figure 5, top right). The

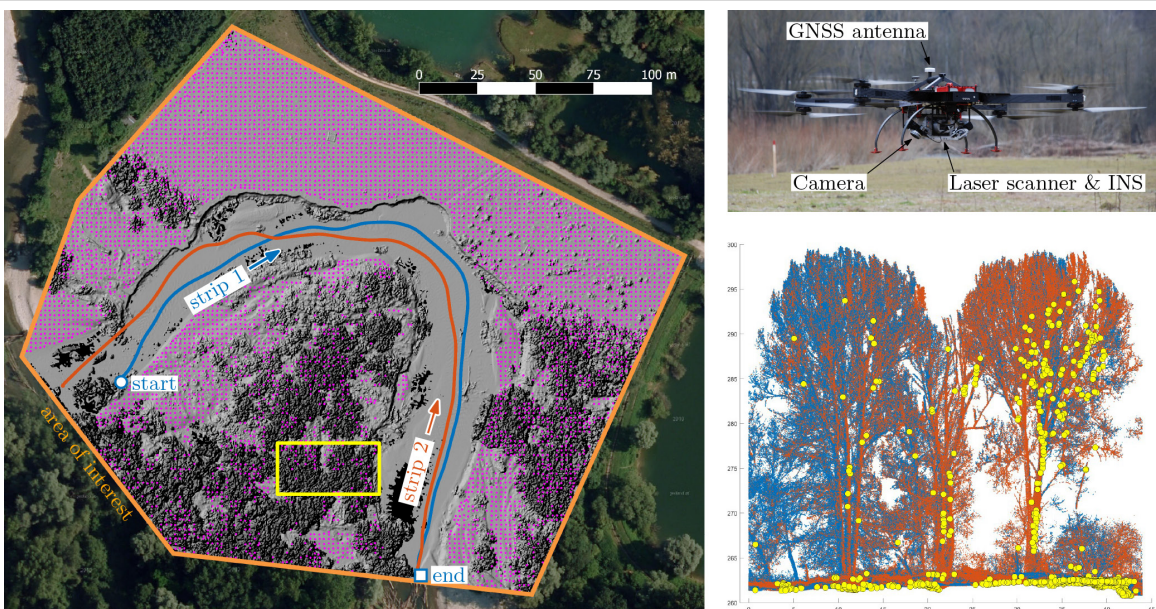


Figure 5. The trajectory correction model is demonstrated on the basis of a single pair of strips (flight trajectories in blue/orange). These two strips were acquired by following the course of the Pielach River in 25 m flying altitude. The magenta points were taken from a simultaneous (manned) ALS campaign and introduced as ground control points into the strip adjustment. The point clouds within the rectangle are depicted at the bottom right corner (yellow points = position of "strip to strip" correspondences in this area). Top right: Riegl RiCopter.

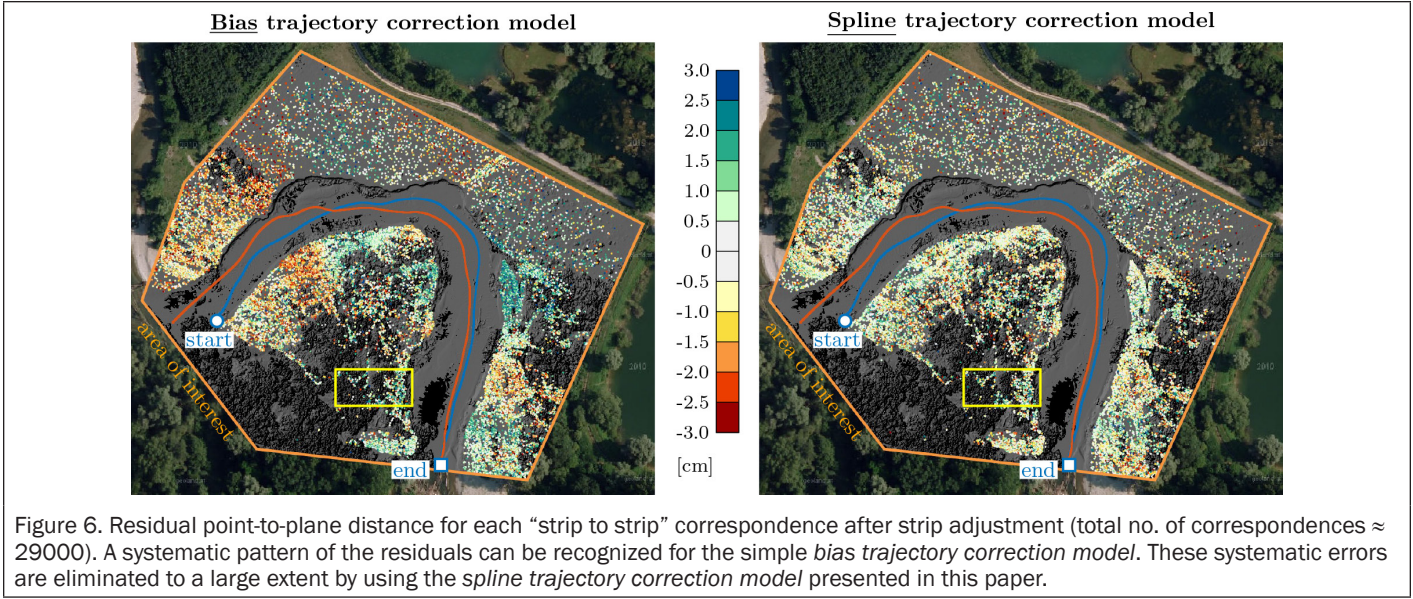


Figure 6. Residual point-to-plane distance for each “strip to strip” correspondence after strip adjustment (total no. of correspondences \approx 29000). A systematic pattern of the residuals can be recognized for the simple *bias trajectory correction model*. These systematic errors are eliminated to a large extent by using the *spline trajectory correction model* presented in this paper.

manufacturer’s specifications about the UAV, the laser scanner, and the GNSS/INS solution are reported in Table 3.

Data capturing was carried out with 14 longitudinal strips, 4 cross strips, and 2 strips along the Pielach river². The regular distance between longitudinal strips was 40 m and the flying altitude was 25 to 50 m above ground. Depending on the sensor-to-target range the resulting laser footprint diameter is 1.0 to 2.5 cm, enabling the detection of small vegetation objects. The UAV was autonomously flying the programmed path (based on waypoints) with a speed of 8 m/s. The mission parameters and the large scanner FOV resulted in a mean laser pulse density of 1,500 points/m², and in multiple strip overlaps so that the vegetation was captured from multiple sides (see Figure 1). The point clouds acquired in this flight campaign were already used in other publications; in Mandlburger *et al.* (2015b) the potential of the data for vegetation modeling was investigated and in Mandlburger *et al.* (2015c) a comparison with ALS and Airborne Laser Bathymetry (ALB) data was presented. For these works, strip adjustment was performed for all strips. However, for a better understanding, the presented *spline trajectory correction model* is demonstrated in the following on the basis of a single pair of strips only (Figure 5).

In this minimal example, we compare the results of the *spline trajectory correction model* and the simple *bias trajectory correction model* (Table 4). With the latter only a bias is estimated for each trajectory element per strip; looking at the Equation 7 and 8, this corresponds to

$$n_{[j]} = 1 \Rightarrow \Delta t = t_{e[j]} - t_{s[j]} \quad (22)$$

$$a_{1[j,k]} = a_{2[j,k]} = a_{3[j,k]} = 0 \quad (23)$$

and the coefficients $a_{0[j,k]}$ is the bias estimated by adjustment.

The two investigated strips were acquired by following the course of the Pielach River in 25m flying altitude. These two strips were later used to investigate short term water level differences, thus a very high strip registration accuracy was required to distinguish signal (i.e., water level differences) from noise. To minimize the discrepancies between these two strips, approximately 29,000 strip to strip correspondences were established, see Figure 6:

- within the overlap volume of the two strips,
- inside the area of interest,

2. An animation of the captured point clouds after strip adjustment can be seen here: <https://youtu.be/GwyNhUjFr2I>

Table 4. Comparison of strip adjustment results for both correction models

	Strip adjustment results	
	Bias TCM	Spline TCM
# parameters		
• scanner calibration	4	4
• mounting calibration	6	6
• trajectory correction	11	504
# observations		
• correspondences		
• strip to strip (Fig. 6, 7)	29180	28662
→ std. dev. residuals	1.83 cm	1.38 cm
→ mean residuals	0.01 cm	0.00 cm
• ground-truth data to strip	7888	7866
→ std. dev. residuals	1.82 cm	1.65 cm
→ mean residuals	0.00 cm	0.00 cm
• coefficients (eq. 19)	0	126
# constraints	0	390
redundancy	37047	36530

- outside the river area due to the water dynamics, and
- only on relatively smooth surface areas (details later).

The Normal Sampling method (Glira *et al.*, 2015a) was used for the selection of the correspondences. Thereby, the correspondences are selected so that the distribution of their normals in angular space (slope versus aspect) is as uniformly as possible. As can be seen in Figure 5 (bottom right), this leads to a broad distribution of the correspondences in 3D object space, i.e., correspondences are not only established on the terrain, but also on thicker stems and branches.

The datum of the strip adjustment was defined by 5,630 homogeneously distributed ground control points, which have been extracted from a simultaneous manned ALS flight campaign (Figure 5, left side). These points were matched with the two overlapping strips, giving in total approximately 7,900 datum-defining ground-truth data to strip correspondences. The large number of ground control points avoid the problem of block deformation, which was discussed in the previous section.

To minimize the point-to-plane distances, the normal vector is needed for each correspondence (see Figure 3). The normal vectors were estimated by considering a maximum

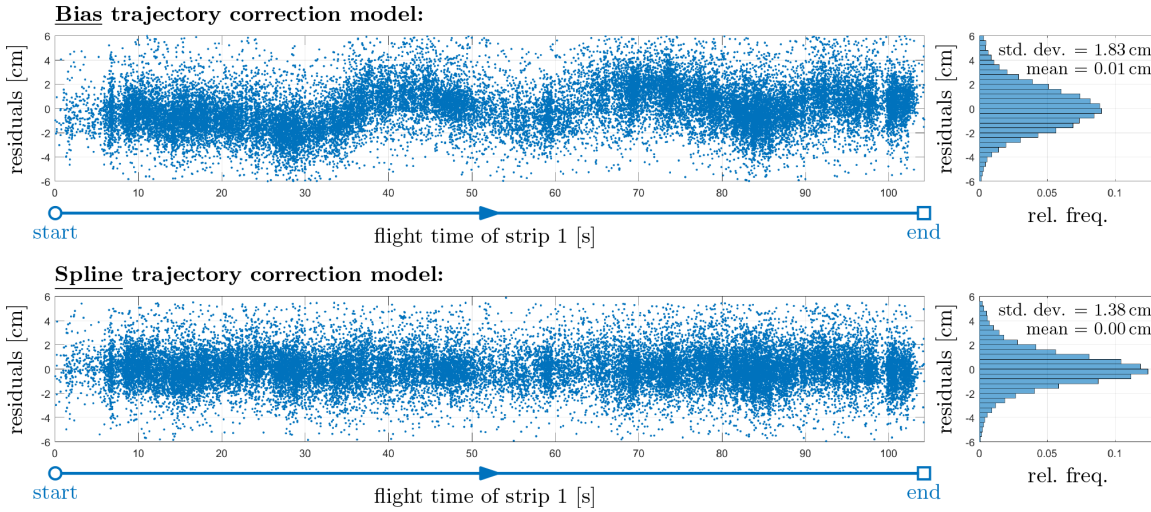


Figure 7. Residual point-to-plane distance for each “strip to strip” correspondence after strip adjustment depending on the flight time of strip 1. *Bias trajectory correction model*: the systematic error pattern in object space (see Figure 6, left) is also clearly visible in time domain. *Spline trajectory correction model*: the residuals are predominantly random distributed, i.e., systematic errors are minimized by the estimated spline functions (see Figure 9).

number of 20 neighboring points within a maximum search radius of 0.5 m. However, if the estimated normal vector is unreliable (i.e., if the standard deviation of the points from the adjusting plane exceeds σ_{\max}), the associated correspondence was rejected. As a result, correspondences are established within relatively smooth areas only (in this example we used $\sigma_{\max} = 2$ cm). All parameters, i.e., the search radius, the number of neighboring points, and σ_{\max} , were chosen empirically by considering the point density, the topography, and the measurement accuracy of the laserscanner (Table 3).

In Figures 6 and 7 the residual point-to-plane distances of each strip to strip correspondence can be inspected in object space and time domain, respectively. As can clearly be seen, using the *bias trajectory correction model* the residuals show a strong systematic pattern, with amplitudes of up to 3 to 4 cm. As these errors are significantly larger than the measurement accuracy of the laser scanner (Table 3), it can be concluded that time dependent trajectory errors are the dominant remaining error source. If we take a closer look at the error pattern in time domain (upper part of Figure 7), it can be recognized that the systematic part of these errors can be well-modeled by smooth and continuous functions, e.g., by cubic splines, as we propose here. Thus, with the *spline trajectory correction model*, the systematic errors could be widely eliminated, leading to residuals that are mainly random distributed over time (lower part of Figure 7). We have chosen in this example a segment length Δt of 10 s for the estimation of the spline correction functions, which leads to 10 segments for strip 1, and 11 segments for strip 2 (Figure 9). By using this correction model, the relative orientation of the strips (defined as standard deviation of the residual point-to-plane distances for all strip to strip correspondences, cf. Table 4) was improved by 25 percent, i.e., from 1.83 cm to 1.38 cm. Accordingly, the absolute orientation of the strips was improved by 10 percent, i.e. from 1.82 cm to 1.65 cm. A comparison with Table 3 shows that these values, as well as the estimated correction functions are widely in conformity with the accuracies declared by the manufacturers.

An appropriate choice of the segment length Δt is of great importance. On the one hand, a too small segment length increases the model complexity without significantly improving the goodness of fit for the model. As can be seen in Figure 8, this applies to $\Delta t < 10$ s in the current case. On the other hand,

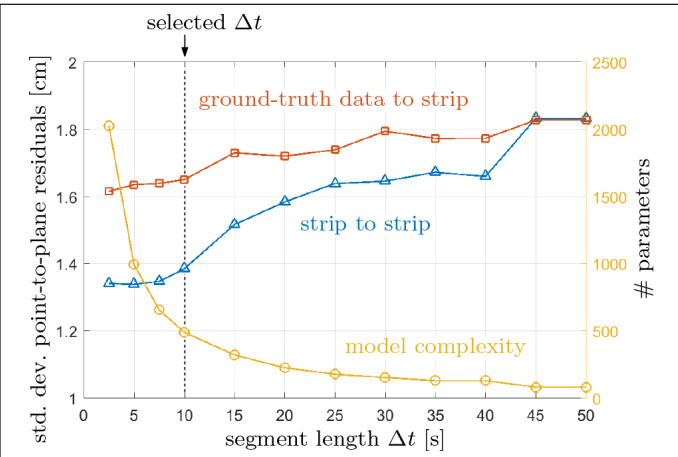


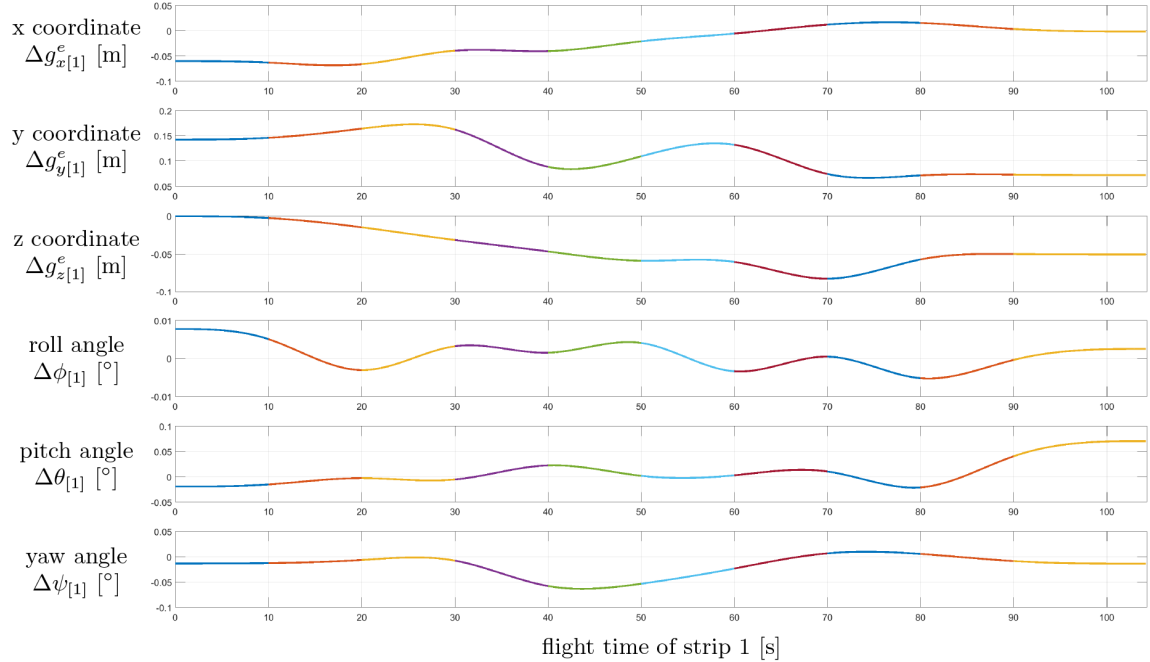
Figure 8. Goodness of fit versus model complexity for different segment lengths Δt .

systematic errors of the trajectory cannot be fully compensated if the segment length is too long. Thus, a good balance between goodness of fit and the complexity of the model, i.e., the number of unknown parameters, has to be established. Several statistical tests can be applied to this purpose, e.g., the Akaike Information Criterion (AIC) or Minimum Description Length (MDL) tests (Burnham and Anderson, 2002). In this example, a good trade-off was found for $\Delta t = 10$ s.

Summary and Outlook

In this article, we extended our previous work on the topic of strip adjustment (Glira *et al.*, 2015a; Glira *et al.*, 2015b) by the estimation of time-dependent trajectory errors. We demonstrated that using the *bias trajectory correction model*, the residual errors primarily originate from the trajectory data. For this, the presented *spline trajectory correction model* can be applied to minimize the effect of an erroneous trajectory on the georeferencing accuracy of point clouds. The trajectory errors are thereby modeled by natural cubic splines with constant segment length in time domain. Additional observations are incorporated into the adjustment to ensure the determinability of the correction functions in areas without redundancy, i.e.,

Trajectory corrections of strip 1



Trajectory corrections of strip 2

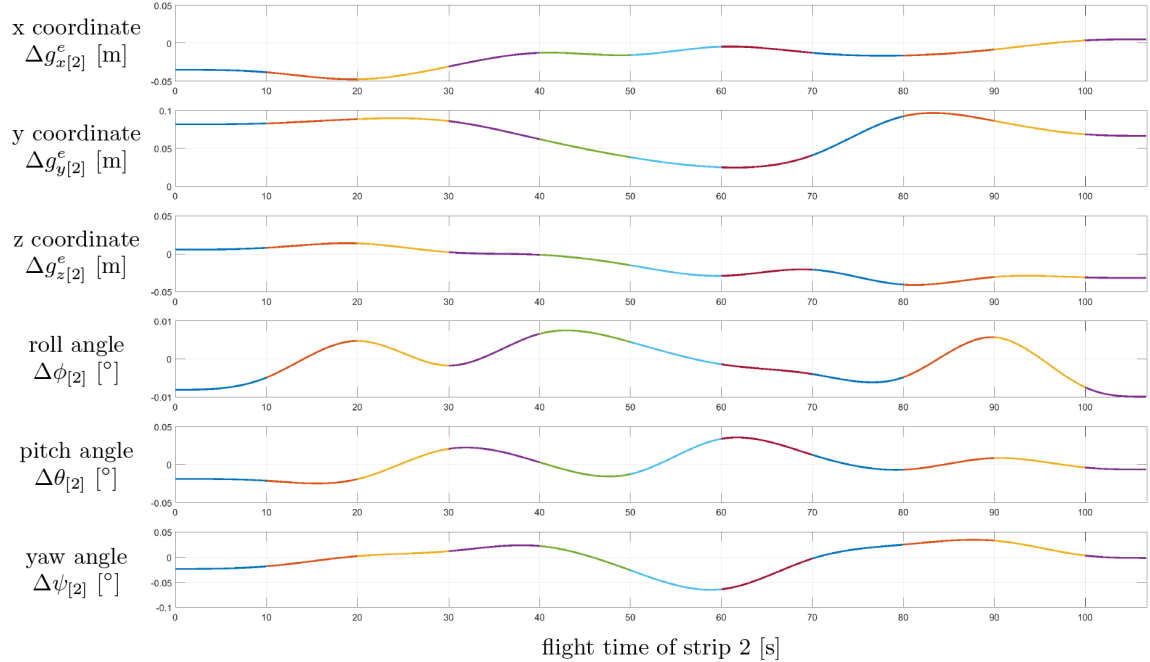


Figure 9. Estimated trajectory correction functions for both strips.

without overlapping strips. Due to its flexibility, the proposed correction model can be used to eliminate almost any systematic discrepancies between overlapping strips; especially if a very small segment length is used. However, this flexibility also implies some risks: if the segment length Δt is too small, an absolute deformation of the ALS block might occur. Thus, the usage of ground-truth data, distributed homogeneously over the whole block, is recommended.

The *spline trajectory correction model* was demonstrated by means of data from an UAV-based laser scanning system.

Such systems use light-weight navigation sensors with a moderate level of accuracy for the estimation of the platform's trajectory. As a consequence, the georeferencing of the point clouds is sub-optimal and should therefore be optimized by strip adjustment. This was demonstrated in a minimal example for a single pair of strips. Extensive ground-truth data was extracted from a simultaneous manned ALS campaign. By means of strip adjustment, the relative and absolute orientation of the strips was improved to 1.38 cm and 1.65 cm, respectively. These results confirm the suitability of the

proposed calibration and correction model, as the adjusted strips are free from systematic errors and the residual random errors widely correspond to the specifications of the deployed measurement system.

The presented strip adjustment method with the *spline trajectory correction model* was already successfully applied to several manned ALS campaigns. As a next step, we want to use the strip adjustment framework, together with the trajectory correction model presented in this paper, to improve the georeferencing of Mobile Laser Scanning point clouds of an urban area.

Acknowledgments

This research was carried out within (a) PROSA (high-resolution measurements of morphodynamics in rapidly changing PROglacial Systems of the Alps), which is a joined project of the German research community (DFG) (BE 1118/27-1) and the Austrian Science Fund (FWF) (I 1647), and (b) the COMET-K project / Alpine Airborne Hydromapping from research to practice, which is funded by the Austrian Research Promotion Agency (FFG).

References

- Bäumker, M., and F. Heimes, 2001. New calibration and computing method for direct georeferencing of image and scanner data using the position and angular data of an hybrid inertial navigation system, *Proceedings of the OEEPE Workshop, "Integrated Sensor Orientation"*, Hannover, Germany.
- Besl, P.J., and N.D. McKay, 1992. Method for registration of 3-d shapes, Robotics-DL tentative, *International Society for Optics and Photonics*, pp. 586–606.
- Burnham, K.P., and D.R. Anderson, 2002. Model selection and multimodel inference: A practical information-theoretic approach, *Springer Science & Business Media*.
- Chen, Y., and G. Medioni, 1992. Object modelling by registration of multiple range images, *Image and Vision Computing, Range Image Understanding*, 10(3):145–155.
- Colomina, I. 2015. On trajectory determination for photogrammetry and remote sensing: Sensors, models and exploitation, *Proceedings of Photogrammetric Week 2015* (D.Fritsch, editor), Stuttgart, Germany, pp. 131–142.
- Colomina, I., and P. Molina, 2014. Unmanned aerial systems for photogrammetry and remote sensing: A review, *ISPRS Journal of Photogrammetry and Remote Sensing*, 92:79–97.
- Ebner, H., W. Kornus, and T. Ohlhof, 1992. Simulation study on point determination for the MOMS-02/D2 space project using an extended functional model, *ISPRS Archives of Photogrammetry, Remote Sensing and Spatial Information Sciences*, Volume 29, pp. 458–464.
- Friess, P., 2006. Toward a rigorous methodology for airborne laser mapping, *Proceedings EuroCOW*, Castelldefels, Spain, pp. 25–27.
- Glira, P., N. Pfeifer, C. Briese, and C. Ressl, 2015a. A correspondence framework for ALS strip adjustments based on variants of the ICP algorithm, *PFG Photogrammetrie, Fernerkundung, Geoinformation*, 2015(4):275–289.
- Glira, P., N. Pfeifer, C. Briese, and C. Ressl, 2015b. Rigorous strip adjustment of airborne laserscanning data based on the ICP algorithm, *ISPRS Annals of Photogrammetry, Remote Sensing and Spatial Information Sciences*, II-3/W5:73–80.
- Gruen, A., and L. Zhang, 2002. Sensor modeling for aerial mobile mapping with threeline-scanner (TLS) imagery, *ISPRS Archives of Photogrammetry, Remote Sensing and Spatial Information Sciences*, XXXIV Part 2:139–146.
- Habib, A., K.I. Bang, A.P. Kersting, and D.-C. Lee, 2009. Error budget of lidar systems and quality control of the derived data, *Photogrammetric Engineering & Remote Sensing*, 75(9):1093–1108.
- Hebel, M., and U. Stilla, 2012. Simultaneous calibration of ALS systems and alignment of multiview LiDAR scans of urban areas, *IEEE Transactions on Geoscience and Remote Sensing*, 50(6):236.
- Hofmann, O., P. Nave, and H. Ebner, 1984. DPS - A digital photogrammetric system for producing digital elevation models and orthophotos by means of linear array scanner imagery, *Photogrammetric Engineering & Remote Sensing*, 50(8):1135–1142.
- Kager, H., 2004. Discrepancies between overlapping laser scanner strips - Simultaneous fitting of aerial laser scanner strips, *International Archives of Photogrammetry, Remote Sensing and Spatial Information Sciences*, 35(B1):555–560.
- Kalman, R.E., 1960. A new approach to linear filtering and prediction problems, *Journal of Fluids Engineering*, 82(1):35–45.
- Mandlburger, G., P. Glira, and N. Pfeifer, 2015a. UAS-borne lidar for mapping complex terrain and vegetation structure, *GIM International*, 29(7):30–33.
- Mandlburger, G., M. Hollaus, P. Glira, M. Wieser, M. Milenkovic, U. Riegl, and M. Pfennigbauer, 2015b. First examples from the RIEGL VUX-SYS for forestry applications, *Proceedings of SilviLaser 2015*, 28–30 September, La Grande Motte, France.,
- Mandlburger, G., M. Pfennigbauer, U. Riegl, A. Haring, M. Wieser, P. Glira, P., and L. Winiwarter, 2015c. Complementing airborne laser bathymetry with UAV-based lidar for capturing alluvial landscapes, *Proceedings of SPIE*, Volume 9637, pp. 96370A–96370A.
- Mikhail, E., and F. Ackermann, 1976. *Observations and Least Squares*, University Press of America.
- Nolan, J., R. Eckels, M. Evers, R. Singh, and M.J. Olsen, 2015. Multi-pass approach for mobile terrestrial laser scanning, *ISPRS Annals of Photogrammetry, Remote Sensing and Spatial Information Sciences*, II-3/W5:105–112.
- Nuechter, A., D. Borrmann, P. Koch, M. Kuehn, and S. May, 2015. A man-portable, IMU-free mobile mapping system, *ISPRS Annals of Photogrammetry, Remote Sensing and Spatial Information Sciences*, II-3/W5:17–23.
- Ressl, C., N. Pfeifer, and G. Mandlburger, 2011. Applying 3D affine transformation and least squares matching for airborne laser scanning strips adjustment without GNSS/IMU4 trajectory data, *Proceedings of ISPRS Workshop Laser Scanning 2011*, Calgary, Canada.
- Skaloud, J., P. Schaer, Y. Stebler, Y., and P. Tomfie, 2010. Real-time registration of airborne laser data with sub-decimeter accuracy, *ISPRS Journal of Photogrammetry and Remote Sensing*, 65(2):208–217.
- Vosselman, G., and H.-G. Maas, 2001. Adjustment and filtering of raw laser altimetry data, *Proceedings of OEEPE Workshop on Airborne Laserscanning and Interferometric SAR for Detailed Digital Terrain Models*, Stockholm, Sweden.